Co-published by
Institute of Fluid-Flow Machinery
Polish Academy of Sciences
Committee on Thermodynamics and Combustion
Polish Academy of Sciences

http://www.imp.gda.pl/archives-of-thermodynamics/

ARCHIVES OF THERMODYNAMICS

Coupled heat, mass and momentum transfer model of a napa cabbage refrigerated storage chamber

Mirosława Kołodziejczyk[a], Kamil Śmierciew[b], Jerzy Gagan[b], Dariusz Butrymowicz[b]*, Paweł Jakończuk[b], Mateusz Pawłowski[b]

[a]PRONAR, R&D Department, Mickiewicza 101A, 17-210 Narew, Poland
[b]Department of Thermal Engineering, Bialystok University of Technology, Wiejska 45C, 15-351, Bialystok, Poland
*Corresponding author email: d.butrymowicz@pb.edu.pl

Received: 30.09.2024; revised: 14.12.2024; accepted: 16.12.2024

Abstract

Results of numerical simulation of heat, mass and momentum transfer in cold storage chambers for vegetables along with experimental validation are presented in the paper. The case of an experimental napa cabbage cold store was analysed. Coupling of processes occurring in the bulk of vegetables and in the air cooler accomplished by means of the user-defined functions in Ansys Fluent are presented. The model combines the cooling capacity with the processes occurring in the bed of cabbage, namely transpiration and respiration, and other heat gains/losses that occur in the chamber. The model of porous media was applied in terms of the bed of vegetables and air cooler. A thermal non-equilibrium model was assumed. The output of simulations were the heat and mass transfer coefficients. The numerical results were compared with the measurements. A good agreement between numerical results and experimental data in terms of temperatures in the bulk of vegetables and relative humidity was achieved. The moisture loss in stored products resulting in total loss of weight was analysed. Good agreement with experimental results and regions of the highest shrinkage of the stored vegetables were indicated.

Keywords: CFD modelling; Heat and mass transfer; Porous model; Cold storage; Napa cabbage

Vol. 45(2024), No. 4, 223–235; doi: 10.24425/ather.2024.152012

Cite this manuscript as: Kołodziejczyk, M., Śmierciew, K., Gagan, J., Butrymowicz, D., Jakończuk, P., & Pawłowski, M. (2024). Coupled heat, mass and momentum transfer model of a napa cabbage refrigerated storage chamber. *Archives of Thermodynamics*, 45(4), 223–235.

1. Introduction

It is estimated by the United Nations Department of Economic and Social Affairs that by 2050 the world's population will increase to 9.3 billion, which will require at least 70% and in some scenarios even a 100% increase in global crop production [1]. This means that the food production needs to increase by 100% and the demand for storage, and related factors—such as climate change, power consumption, hunger and land use—are expected to rise accordingly [2]. The need for refrigerated storage of fruits and vegetables causes significant energy consumption and greatly influences the cost of postharvest handling of agricultural products.

Inappropriate storage conditions in the cold storage chambers may generate drying of the product and under too low temperatures may cause the products injury that strongly deteriorates the quality of the stored products. Losses may occur mainly due to non-uniformity of the environmental conditions inside the bed of the stored products. The most important factors that protect the product against damage are air temperature, air velocity and air humidity. Important are also load arrangements and physical properties of vegetables and fruits. The macroscopic

Nomenclature

A_{fs} – heat transfer surface area, m^2
c_p – specific heat, J/kgK
C_2 – resistance coefficient
$D_{i,m}$ – mass diffusion coefficient
E – total fluid phase energy, J/kg
$\vec{g}$ – gravitational acceleration, m^2/s
h – convective mass transfer coefficient
$\vec{J}_i$ – diffusion flux vector
k – thermal conductivity, W/(m K)
L – latent heat of evaporation/condensation, J/kg
Le – Lewis number
$\dot{m}$ – transpiration rate, kg/s
Nu – Nusselt number
p – pressure, Pa
Pr – Prandtl number
R_v – water vapour gas constant, J/(kg K)
RH – relative humidity, %
$\dot{Q}$ – cooling capacity, kW
Sc – Schmidt number
$\vec{S}$ – body force term
t – time, s
t, T – temperature, K
V – volume, m^3
V – magnitude of velocity, m/s
$\vec{V}$ – velocity vector
W – heat generation, W/kg
Y_t – species mass fraction

Greek symbols

α – permeability of porous medium
β – interfacial area density, kg/m^3
δ – relative difference, %
Δl – length, m
Δp – static pressure jump across the fans, Pa
ε – porosity
η – effectiveness
μ – dynamic viscosity, Pa·s
ρ – density, kg/m^3

Subscripts and Superscripts

a – air
f – fluid
p – pressure
s – solid
t – turbulent
v – vapour
w – wall

Abbreviations and Acronyms

CAD – computer-aided designed
CFD – computational fluid dynamics
RANS – Reynolds-averaged Navier-Stokes
RNG – re-normalization group
SAS – scale adaptive simulations
SIMPLE – semi-implicit method for pressure linked equations
SST – shear stress transport
UDF – user-defined functions
VPL – vapour pressure lowering

energy balance approach cannot give the answers to the questions how these factors influence the local temperature and relative humidity inside the bulk and where in the bulk warm and cold zones are placed, causing excessive drying or chilling injuries of the vegetable tissue. In light of this fact, numerical modelling of the air conditions in the cold storage chambers seems to be the best approach in examining the reasons for unfavourable heterogeneity of thermal and flow parameters inside the bulk. Therefore, numerical modelling of the cold storage chamber may be attractive for its cost-saving potential and ability to adapt to different model parameters quicker than e.g. experimental investigations. In fact, numerical modelling using CFD (computational fluid dynamics) approach allows us to fully understand the complexity of biological systems. For this reason, the CFD approach became the basic tool that allows replicating and predicting phenomena in physics, chemistry and biology [3]. The variety of CFD applications related to heat and mass transfer in adsorption packed beds [4], cold storage rooms [5], and drying beds can be found in the literature. The papers [6–8] provided analysis of air flow and heat transfer through the package design. The aspects of energy consumption and savings are presented in papers [9,10]. The operation of the cooler is the major factor that influences the storage conditions. The forced-air cooling units for the cold storage chambers are usually mounted just under the ceiling of the chamber and they are equipped with several fans and the air cooler. The evaporator of the refrigeration system or alternatively the heat exchanger for glycol cooling installations may be applied as air coolers. Its thermal performance depends on the storage conditions and should be analysed together with the entire chamber with its load as one computational task. This may be thought as a challenge for a wide range of geometric scales of the modelled objects in the analysed cold store. The entire geometry consists of empty spaces filled with humid air only, however, there are also large areas in which a large number of small objects exist, i.e. pieces of products located inside the boxes or palloxes as well as elements of the cooling unit (fins and tubes of the air cooler). It is a challenging and time-consuming task from the pre-processing and simulation point of view to build a geometric model of the cold storage chamber which retains the exact shape of all these relatively small details. For that reason, a porous media model with large pores is widely used in modelling the bed of products and the air cooler. Using the porous model is a reasonable compromise between the computational cost and accuracy of the results [11, 12]. A space occupied by a large number of small objects is treated as a fictitious continuum of resistance to flow that is equal to the resistance of real objects. This is taken into account by means of the additional negative source term in the momentum equation. The containers of vegetables are usually modelled by a packed bed approach including both viscous and inertia resistance calculated according to the Ergun equation, which was demonstrated for the packed bed of apples [13] with the use of

the Brinkman-modified Ergun equation. In paper [14] with the use of the Ergun equation, an average accuracy of 20% on the velocity magnitudes was observed on the basis of own experimental data. The effects of blowing duct on ventilation homogeneity around stored products were analysed experimentally and numerically using the Ergun equation in [15]. However, there are also works in which the containers were treated as impenetrable solid areas with specified boundary conditions on the walls [16]. There are also works where the resistance of the bed is calculated on the basis of the experimental data for an enclosure loaded with slotted pallets [17] and inside slotted obstacles in a ventilated enclosure [18].

There are also additional problems associated with the complex geometry of the flow through the containers with stored products. The confinement effect of the porous medium, causing different flow conditions in the vicinity of the walls and inside the bed core as well as narrow gaps between the containers cause a strong increase in the number of computational cells. Both problems were studied by Moureh et al. for refrigerated trucks [19], a slot-ventilated enclosure partially loaded with vented boxes filled by spherical objects [20–22]. Near the wall, the porosity is higher which causes higher velocity gradients than inside the core of the porous medium. The common approach is based on the ratio of the hydraulic diameter to the geometric scale of the pores. Therefore, if this ratio is greater than 10, then the impact of the wall on the flow through the bed can be neglected. The interstices between the boxes in the bulk can be included by increasing the porosity, which can be considered as the additional (fictitious) aerodynamically equivalent porous medium with laminar flow that requires a much smaller number of computational cells than for real gaps [17,21]. Another problem is associated with slotted walls of boxes which are usually modelled as equivalent resistance obtained from the measurements [18,20,21]. One more approach to possible geometric simplification commonly applied is the use of symmetry of geometry [23,24]. However, such a simplification is assumed even though the real flow in such complex geometries is always non-symmetrical.

The air cooler is usually modelled by means of simplified geometry and physics. The fans that force air flow inside the chamber may be taken into account in the model by many different methods, mostly as infinitely thin plates with a given pressure jump in 3D problems [25,26], or alternatively as line segments in 2D problems [27]. In the earlier work of Hoang et al. [16], the changes in pressure in the fan and in the air cooler were modelled. The performance curve of the fan and the resistance curve of the cooler were applied in order to obtain the operation point of the fan, neglecting thus the effect of the chamber. In the paper by Nahor et al. [14], the fan and the cooler were represented by distributed body forces and resistance that was taken from the characteristics of these devices and applied to the block of air cooler dimensions. Hoang et al. [5] modelled the swirling air jets blown out by the fans by means of both nominal data and the measurements of air velocity at the fans outflows. The varying supply air temperature was modelled by the exponential function with adjustments taken from the measurements. Heat transfer in the air cooler is modelled in various ways. Hoang et al. [16] considered only the airflow in the chamber assuming temperature to be constant across the room. In the work [27], the square-shaped fins of the evaporator in 2D simulation were assumed to be at a constant temperature obtained from the measurements. Nahor et al. [14] incorporated a lumped model of heat transfer between the air cooler and the air. Delele et al. [25,26] considered the cooler as a porous medium. The model includes losses due to wall friction. Acceleration and deceleration effects as well as entrance and exit conditions were also included. Cooling capacity and condensation/evaporation effects in the air cooler were also incorporated into the model.

A thermal equilibrium is usually assumed when heat transfer in the bulk of products is modelled. Thus, the difference in temperature between the products and humid air is neglected as in papers [25–27]. Nahor [14] applied the thermal non-equilibrium approach in which the temperature difference between products and cooling air was taken into account. However, the heat transfer model used in this case neglects the thermal conductivity in the bulk. The temperature difference was also taken into account in the paper [28] in which the multi-scale model was applied including conduction inside the separate products, but heat conduction in a bed of vegetables was neglected there. Hoang et al. [5] achieved good agreement between numerical and experimental investigations. The conduction in the separate products was also included by modification of the heat transfer coefficient with the aid of additional internal resistance.

In the present study, a model is formulated for the air flow, heat, mass and momentum transfer in the storage chamber of napa cabbage. This model was verified with the use of own experimental data during long-term storage tests. Due to specific properties of napa cabbage, the coupling of heat and mass transfer as well as flow resistance processes are thought of as a novel contribution to the state of the art in modelling the refrigerated storage of foodstuff. In this approach, the cooling unit and the bulk of vegetables were considered as a whole. The aim of the calculation is the prediction of the non-uniformity of velocity, temperature and humidity distributions that consequently enables the identification of the unfavourable storage conditions, i.e. too high, too low air velocity, temperature or relative humidity. These non-uniformities were validated experimentally. In order to include the close relationship between the phenomena occurring inside the stored vegetables and in the air cooler, the user-defined functions (UDF) in Ansys Fluent were used [29].

2. Description of the model

The experimental cold store chamber of the Research Institute of Horticulture in Skierniewice, Poland, was used for the analysis with the help of a CFD model. Figure 1 shows the photo of the investigated experimental storage chamber seen from the cooler side. The CAD (computer-aided designed) model of the chamber is presented in Fig. 2, and the CAD model of the air cooler – in Fig. 3. The overall dimensions of the cold storage chamber were 2.05 m × 4.33 m × 2.93 m. The geometry of the antechamber is presented in Fig. 2. The chamber was loaded with 2940 kg of products. The napa cabbage was packed in plastic boxes placed on wooden pallets. The basic arrangement of the boxes is a block of dimensions 1.8 m × 2.8 m × 2.17 m. The

block occupies most of the chamber space. As it is seen in Fig.2, the boxes are also stored in the antechamber. The ceiling-type air cooler of a nominal thermal capacity of 1148 W and air flow rate of 1105 m^3/h was connected to the indirect cooling system operating with glycol solution. The continuous, non-stop flow

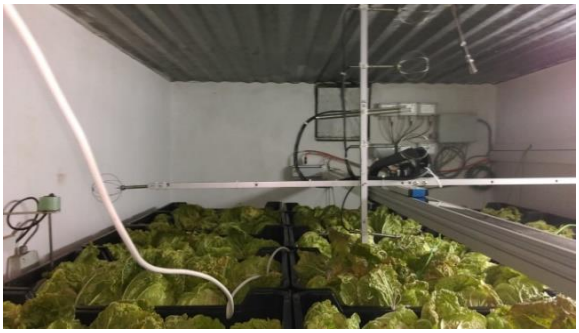

Fig. 1. Photo of the experimental cold store: view from the air cooler side. The elements of the mobile measurement system are visible.

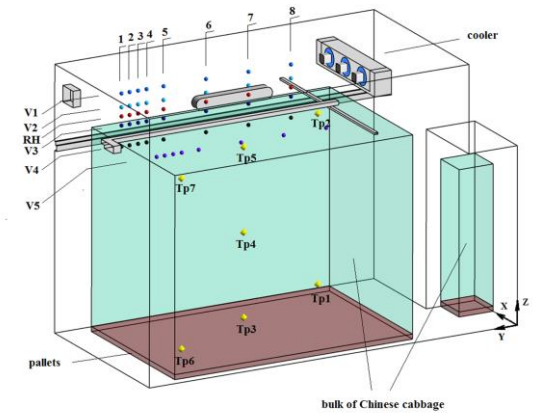

Fig. 2. Geometry of the cold storage chamber along with the antechamber. The points of the measurement system grid are shown (*V* – velocity; RH – relative humidity); *Tp* denotes temperature measurement locations in the vegetable bulk.

of air was provided by three axial fans of 0.2 m of diameter rotating at 1300 rpm, placed at the outflow of the cooler.

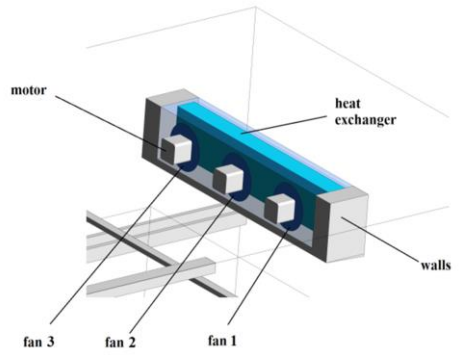

Fig. 3. Geometry of the applied air cooler.

Optimum storage conditions for napa cabbage are: temperature in the range 0°C − +3°C, however, as close as possible to 0°C without freezing is preferred, and the range of relative humidity between 95% and 98%. In order to take into account variable moisture content, the species transport method without chemical reactions was applied in modelling. Humid air was treated as a mixture of oxygen, nitrogen and water vapour. The air was considered an ideal incompressible gas. The physical properties of the air depend on temperature only with coefficients taken from the Fluent library [29].

The flow through the bulk of napa cabbage, heat exchanger in the cooling unit, and wooden pallets with supporting boxes with vegetables were modelled with the use of the porous medium model. Moist air constituted the fluid zone in all regions filled with the porous medium, but the solid zones were formed from different materials depending on the case: cabbage for the bulk of vegetables, aluminium for the air cooler, and wood for the pallets. Properties of aluminium and wood were taken from the Fluent library [18]. Thermophysical properties of napa cabbage (specific heat and thermal conductivity) were obtained through the own measurements performed for the assumed storage temperature of 1°C. The density of cabbage was determined by Bohojło-Wiśniewska [30]. Detailed numerical data are given in Table 1.

3. Mathematical model

The mathematical model of flow in a storage chamber of vegetables includes basic conservation equations with additional equations presented in the next part of this section. The model includes two energy equations for fluid and solid zones of porous media for the dual cell approach or one – for the thermal equilibrium model, and two species transport equations for oxygen and water vapour.

The continuity equation for humid air is as follows:

$$\frac{\partial(\varepsilon\rho)}{\partial t} + \nabla\cdot\left(\varepsilon\rho\vec{V}\right) = 0, \tag{1}$$

where: ε − porosity (for empty space outside the porous material $\varepsilon = 1$), ρ − density of the mixture of oxygen, nitrogen and water vapour as components of humid air, $\vec{V}$ – velocity vector.

The conservation of momentum for incompressible fluid with natural convection is as follows:

$$\frac{\partial(\varepsilon\rho\vec{V})}{\partial t} + \nabla\cdot\left(\varepsilon\rho\vec{V}\vec{V}\right) = \left(\rho - \rho_0\right)\vec{g} - \varepsilon\nabla p + \nabla\cdot\left(\varepsilon\mu\left(\nabla\vec{V} + \nabla\vec{V}^{\mathrm{T}}\right)\right) - \vec{S}, \tag{2}$$

where: p − air pressure, $\vec{g}$ − gravitational acceleration, ρ_0 − operating density, μ − viscosity of moist air including turbulent viscosity, $\vec{S}$ – body force term due to the loss of momentum in the porous medium.

Two transport equations of oxygen and water vapour are taken into account:

$$\frac{\partial}{\partial t}(\rho Y_i) + \nabla\cdot\left(\rho\vec{V}Y_i\right) = -\nabla\cdot\vec{J}_i + S_i, \tag{3}$$

Table 1. Model parameters.

Parameter	Unit	Value
Bulk of napa cabbage		
Density of a cabbage head	kg/m³	568
Specific heat	J/(kg·K)	3955
Thermal conductivity	W/(m·K)	0.4425
Number of cabbages in one box		12–13
Number of boxes in the main bulk		147
Volume of the bulk	m³	11.06
Mass of cabbage in the main bulk	kg	2940
Bulk porosity		0.532
Interfacial area density	m²/m³	7.95
Viscous resistance	1/m²	2777181
Inertial resistance	1/m	412.56
Air cooler		
Volume of heat exchange	m³	0.0189
Heat exchange surface area	m²	5.703
Surface efficiency under wet conditions		0.81
Porosity		0.60
Viscous resistance	1/m²	1.5×10^7
Inertial resistance	1/m	92.468
Interfacial area density	m²/m³	301.75
Fan power	W	3×10
Fan speed, rpm	1300	
Pallets		
Height	m	0.055
Porosity		0.99
Inertial resistance	1/m	1
Material		wood
Walls		
Overall heat transfer coefficient	W/(m²K)	0.25
Wall thickness	m	0.3
Free stream temperature	°C	12

where i is the indicator of the species (oxygen or water vapour), Y_i is the species mass fraction, $\vec{J}_i$ – diffusion flux; S_i – rate of species creation, taking a non-zero value only for water vapour. The nitrogen mass fraction is calculated as a supplement to unity.

In turbulent flows, the diffusion flux can be described as, Ansys Fluent [29]:

$$\vec{J}_i = -\left(\rho D_{i,m} + \frac{\mu_t}{\mathrm{Sc}_t}\right)\nabla Y_i - D_{T,i}\frac{\nabla T}{T}, \quad (4)$$

where: $D_{i,m}$ – mass diffusion coefficient; μ_t – turbulent viscosity; Sc_t – turbulent Schmidt number, $D_{T,i}$ – turbulent diffusivity, T – temperature.

Vegetables and fruits during postharvest storage are still living organisms, so metabolic processes occur. The most important of them that affect heat and mass balance in the cold storage chamber are the respiration and transpiration processes. In order to include the heat generation inside a porous medium, which is the bulk of vegetables, but also the heat exchanger, solid and fluid phases are not in thermal equilibrium. Furthermore, napa cabbage heads are relatively large in size and the differences in temperature between the solid and fluid phases of the porous medium making the bulk cannot be neglected. For that reason, the non-equilibrium model of heat transfer in the porous medium (a dual cell approach) was used assuming that the solid zone of the porous medium is spatially coincident with the fluid zone, and two equations of energy, for humid air (5) and for the solid material (6), are solved separately:

$$\frac{\partial(\varepsilon\rho E)}{\partial t} + \nabla\cdot\left[\vec{V}(\rho E + p)\right] = \nabla\cdot\left[k\nabla T - \sum_i h_j J_j + \left(\bar{\bar{\tau}}_{eff}\cdot\vec{V}\right)\right] + S_f^h + h_{fs}\beta_{fs}(T - T_s), \quad (5)$$

$$\frac{\partial[(1-\varepsilon)\rho_s E_s]}{\partial t} = \nabla\cdot[(1-\varepsilon)k_s\nabla T_s] + S_s^h + h_{fs}\beta_{fs}(T_s - T), \quad (6)$$

where $\bar{\bar{\tau}}_{eff}$ is the stress tensor. The above equations are connected by the heat transferred through the fluid/solid interface. Source terms in both equations represented by Newton's law describe this connection. This requires heat transfer coefficients h_{fs} to be determined. The symbol β_{fs} stands for the interfacial area density. The meaning of other terms in energy equations is as follows: E and E_s – total fluid and solid phase energy, ρ_s – density of the solid matrix, k and k_s – fluid and solid thermal conductivity, T and T_s – temperature of the fluid and solid phases, respectively, S_f^h and S_s^h – energy sources terms in fluid and solid zones, which will be defined in the next part of this section. This model of heat transfer in the porous medium was applied for the bulk of vegetables and for the heat exchanger. The wooden pallets which supported the boxes with vegetables, because of a very high porosity of this region, were also treated as the porous medium, but using the equilibrium single-phase porous medium model.

In modelling the flow physics, the geometry of the cooling unit was simplified to the heat exchanger considered as a box of porous medium (shown in blue in Fig. 3), and fans being infinitely thin plates with a pressure jump (shown in dark blue in Fig. 3). The pressure jump depends on the local normal velocity component according to the fan performance curve:

$$\Delta p = -0.085\,V_n^3 + 1.9046\,V_n^2 - 14.998\,V_n + 60.604, \quad (7)$$

where Δp is the static pressure jump across the fans and V_n is the local normal velocity.

The jets of air from the fans were visualised using fibre tufts. The measurement allows for modelling the performance of the fans more completely. The divergent cones of air blown out by the fans were observed. The angle of divergence was close to 90°. The inclination angle of the velocity vector was about 10°. Based on these results, the radial and tangential components of velocity were defined.

In both cases of flow through the cabbage bulk and the heat exchanger, a porous medium was considered to be an isotropic material with the loss of momentum S expressed by a pressure gradient ∇p [29]:

$$S = \nabla p = \frac{\Delta p}{\Delta l} = \frac{\mu}{\alpha}V + \frac{1}{2}C_2 V^2. \quad (8)$$

The first term on the right-hand side of Eq. (8) is the viscous resistance; μ is the viscosity, α – permeability of the porous medium; V – magnitude of the velocity. The second term is the inertial resistance which contains the resistance coefficient C_2. These terms – the heat exchanger permeability α and inertial resistance coefficient C_2 were obtained from performance curves calculated by Śmierciew et al. [31] through numerical simulations of the flow and corresponding pressure drop in the actual cooling unit of the width of heat exchanger Δl = 0.09 m. The bed of vegetables was modelled as a porous medium. For the derivation of pressure loss coefficients due to viscosity and inertia, a series of experimental investigations were conducted in a controlled wind channel with napa cabbage [32]. The napa cabbage bulk characteristic curve was obtained based on the pressure drop measurements for several mean velocities on the length of the bed Δl = 0.6 m. The permeability α of the bed and its inertial coefficient C_2 were computed from Eq. (8). The results for the heat exchanger and cabbage bed are collected in Table 1.

Transpiration and water vapour condensation processes have an influence on the moisture content in the air in the cold storage chamber. As previously stated, the napa cabbage is stored in the range of temperatures between 0°C and 3°C under a relative humidity (RH) range of 95–98%. Therefore, there may appear some spots in the chamber where the condensation process occurs, both, in the heat exchanger and at the vegetable surface. The model of evaporation and condensation processes was incorporated into the proposed modelling approach. This model consists of the spatial distribution of volume water vapour sources or sinks in the regions modelled as porous media (cabbage bulk and heat exchanger). As a consequence, thermal effects of phenomena such as transpiration, condensation and respiration were also represented by the volumetric sources.

The model of evaporation/condensation in the bulk assumed that the process is driven by a difference between the water vapour pressure in the boundary layer at the surface of a vegetable and in the surrounding air [33]. The transpiration rate defined as a mass flow rate of moisture transpired per surface area of a vegetable can be expressed as follows:

$$\dot{m} = k_t(\mathrm{VPL}\, p_{sat} - p_v), \tag{9}$$

where: VPL$p_{sat} - p_v$ means the deficit in the water vapour pressure. Because of dissolved substances, the vapour pressure at the vegetable surface is lower than the saturation pressure at the vegetable surface temperature p_{sat}. The vapour pressure lowering coefficient VPL was evaluated after Becker et al. [33] at 0.99. The transpiration coefficient k_t and the convective mass transfer coefficient h_a are related by the perfect gas law:

$$k_t = \frac{1}{R_v T} h_a, \tag{10}$$

where: T – local absolute temperature of the boundary layer; R_v – water vapour gas constant. The Lewis relationship can be used for the calculation of the convective mass transfer coefficient h_a, assuming that the Lewis number Le = 1,

$$h_a = \frac{h_{tc}}{\rho c_p \mathrm{Le}^{2/3}}, \tag{11}$$

where ρ is the humid air density, c_p is the specific heat of humid air and h_{tc} can be calculated from the correlation for low velocity force convection in a packed bed of spheres [34]. This correlation was applied also by Nguyen et al. [35] for the prediction of water loss for pears. Thus, the dimensionless relationship describing the convective heat transfer is as follows:

$$\mathrm{Nu} = 2.19\, \mathrm{Re}^{0.33}\, \mathrm{Pr}^{0.33} \tag{12}$$

with the definition of Nusselt number Nu as follows:

$$h_{tc} = \frac{\mathrm{Nu}k}{d_{pe}}, \tag{13}$$

where h_{tc} is the convective heat transfer coefficient, k denotes the thermal conductivity of moist air and d_{pe} – diameter of the sphere with a volume equal to the actual volume of a vegetable.

The process of transpiration/condensation in the bulk of vegetables was introduced into the model by transpiration rates distributed along the volume of the bed, in kg/(m^{3}s):

$$S_v = \pm \dot{m}\, \beta, \tag{14}$$

where $\dot{m}$ is calculated by Eq. (9). The positive sign is used for the transpiration process, and the negative one for the condensation process. The symbol β denotes the interfacial area density. The thermal effect of the process is also modelled as a volumetric heat source/sink by the following formula:

$$E_v = -S_v\, L, \tag{15}$$

where the latent heat of evaporation/condensation L is considered as a function of temperature T as follows [36]:

$$L = C_1\, T^2 + C_2\, T + C_3, \tag{16}$$

where C_1 = 0.0091×10^3, C_2 = –7.5129091×10^3, and C_3 = 3875.1×10^3. Sources due to evaporation and condensation were distributed in the fluid phase of the porous medium.

Becker and Fricke [37] related the heat generation rate due to respiration, expressed in W/kg, to the temperature from the carbon dioxide production correlation:

$$W = \frac{10.7f}{3600}\left(\frac{9}{5}t + 32\right)^g. \tag{17}$$

Here, t is the temperature in °C. The coefficients are: f = 6.0803×10^{-04}, g = 2.6183 [38]. Heat of respiration was distributed in the solid phase of the porous medium (cabbage) as volumetric sources and calculated in the following manner:

$$E_r = \frac{Wm}{V}, \tag{18}$$

where m denotes the mass of cabbage in the chamber and V is the volume of the bulk.

The model of heat and mass transfer in the heat exchanger was based on the cooling capacity including the sensible $\dot{Q}_s$ and latent $\dot{Q}_l$ heat transfer rates:

$$\dot{Q} = \eta\left(\dot{Q}_s + \dot{Q}_l\right) \tag{19}$$

with the overall surface efficiency η under wet conditions evaluated after Ma et al. [39] at 0.81. The air side sensible heat transfer rate was calculated from Newton's law:

$$\dot{Q}_s = h_{tx} A_{fs} (T - T_{sat}), \tag{20}$$

where: h_{tx} – air side heat transfer coefficient; A_{fs} – heat transfer surface area, T – temperature of moist air (of the porous medium modelling the heat exchanger), T_{sat} – temperature in the boundary layer at the surface of the solid phase (coils and tubes) of the heat exchanger under saturation conditions.

Condensation in the air cooler was modelled in a similar way as evaporation/condensation in the bulk of vegetables. The water vapour condensation rate was calculated using Eq. (9) with VPL = 1. Following this assumption, the latent heat transfer rate can be expressed as:

$$\dot{Q}_l = k_{tx} A_{fs} (p_v - p_{sat}) L, \tag{21}$$

where: p_v – vapour pressure of surrounding air; p_{sat} – pressure in the boundary layer at the solid surface under saturation conditions. The coefficient of condensation in the heat exchanger k_{tx} was calculated similarly as for vegetables using Eqs. (10) and (11). Volumetric water vapour sinks and corresponding condensation heat sources were modelled following Eqs. (14) and (15) and distributed in the fluid phase of the heat exchanger.

The convective heat transfer coefficient h_{tx} on the air side can be calculated from the total heat transfer rate $\dot{Q}$ according to Eqs. (19)–(21) as

$$h_{tx} = \frac{\dot{Q}}{\eta A_{fs} \left[(T_a - T_{sat}) + \frac{L}{R_v T_a \rho c_p \mathrm{Le}^{2/3}} (p_v - p_{sat}) \right]}, \tag{22}$$

provided that the total cooling capacity $\dot{Q}$ can be evaluated experimentally or provided by the manufacturer.

Local flow parameters should be the basis for determining the heat transfer coefficients in the bulk of vegetables [40]. According to this suggestion, in this paper, all quantities describing the heat transfer in the cabbage bulk, heat of respiration rate and the heat exchanger itself were distributed in space. The actual quantities of the flow are provided by the solver. Subsequently, all sources of heat and mass in the vegetable bulk and in the heat exchanger were treated as field variables. Eventually, it became possible to compute the required cooling capacity $\dot{Q}$ basing on the actual macroscopic heat balance.

The macroscopic heat balance in the cooler, adopted for this work, can be expressed by the formula

$$\dot{Q} = \dot{Q}_t + \dot{Q}_r + \dot{Q}_k + \dot{Q}_w, \tag{23}$$

where: $\dot{Q}$ – cooling capacity, $\dot{Q}_t$ – total heat flux due to transpiration/condensation in the vegetable bulk, $\dot{Q}_r$ – total heat flux due to respiration of vegetables in the bulk; $\dot{Q}_k$ – heat flux due to convection in the air cooler resulting from the temperature difference in the chamber and in the cooler, $\dot{Q}_w$ – total heat flux gain/loss through external walls.

The total heat flux due to transpiration/condensation processes $\dot{Q}_t$ in the vegetable bulk was determined by summing up the bulk heat of transpiration/condensation sources through all computational cells of the fluid phase E_v^i calculated according to Eq. (15) with the cell volumes V_i:

$$\dot{Q}_t = \sum_i E_v^i V_i. \tag{24}$$

The total heat flux due to the respiration process of vegetables was computed in a similar manner:

$$\dot{Q}_r = \sum_i E_r^i V_i, \tag{25}$$

where E_r^i is the volumetric respiratory heat source calculated from Eq. (18) at cell i; and V_i is its volume. The summing is performed through all cells of the solid zone of the cabbage bulk.

The negative source of the cooling capacity was distributed along the cells of the solid phase in the heat exchanger treated as a porous medium according to the formula

$$E_{xt} = -\frac{\dot{Q}}{V_{xt}}, \tag{26}$$

where $\dot{Q}$ is computed according to Eq. (23) and V_{xt} is the volume of the heat exchanger. The value of heat flux $\dot{Q}$ is updated at each iteration of the solution.

Condensation on the coils and fins of the heat exchanger was modelled by spatially distributed negative sources of water vapour given by

$$S_{conxt} = -\max \begin{cases} S_{conxt1} = k_{tx} (p_v - p_{sat}) \beta_{xt} \\ S_{conxt2} = \frac{1}{V_{xt}} \sum_i S_v^i V_i \end{cases}, \tag{27}$$

where $\beta_{xt} = A_{fs}/V_{xt}$ is the interfacial area density in the heat exchanger. The term S_{conxt1} denotes the volumetric condensation rate in the cooler and S_{conxt2} denotes the volumetric source of water vapour generated in the whole bulk of the heat exchanger. The summing in S_{conxt2} is performed through all V_i cells of the fluid zone of the cabbage bulk, and S_v^i is computed according to Eq. (14). This method of determination of the condensation process in the cooler prevented us from an uncontrollable growth of moisture content in the chamber above 100%, which sometimes can occur during the simulation, especially at an initial period.

The governing equations Eqs. (1)–(6) were transformed to RANS equations with the k–ω SST (shear stress transport) turbulence closing equations. The detailed turbulence model equations are given in Ansys Fluent [29], and for this reason, they are not presented in the paper.

A computational grid of 22.7 million control volumes was obtained in Ansys 16.0 using the *cut cell* method. The pressure-velocity coupling was modelled using the SIMPLE (semi-implicit method for pressure linked equations) algorithm.

4. Results and discussion

The experimental investigations were carried out during the post-harvest storage. These studies allow for obtaining data concerning distributions of important parameters required by the computational model. The database includes distributions of velocity, temperature and relative humidity of air. The measurements of air velocity and relative humidity were carried out in the mid-plane of the chamber located at X = 0.99 m above the

vegetable bulk and on one level near the wall located at X = 0.25 m using the mobile measurement system which is seen in Fig.1. As seen in Fig. 2 the velocity and humidity sensors were moved between the points of the measurement grid. The velocity magnitude was measured at elevations denoted as $V1$–$V5$ and the relative humidity was measured at RH level. The data were collected at 8 verticals with a frequency of 1 Hz during 10 min of rest at each position. For the air temperature measurements inside the bulk of cabbages, 7 representative points were selected as shown in Fig. 2. The details of the grids are presented in Tables 2 and 3 with respect to the system of coordinates shown in Fig. 2.

The magnitude of the velocity vector was measured using

Table 2. Dimensions of the measurement grid of a mobile system.

Level						
	V1	*V2*	*RH*	*V3*	*V4*	*V5*
X **(m)**	1.01	1.01	1.01	1.01	1.01	0.25
Z **(m)**	2.88	2.73	2.63	2.53	2.3	2.41

Vertical							
	1	2	3	4	5	6	7
Y **(m)**	4.11	4.015	3.915	3.815	3.615	3.115	2.615

Table 3. Dimensions of the measurement grid in the bulk of vegetables.

Point							
	Tp1	*Tp2*	*Tp3*	*Tp4*	*Tp5*	*Tp6*	*Tp7*
X **(m)**	1.61	1.61	1.01	1.01	1.01	0.41	0.41
Y **(m)**	1.47	1.47	2.67	2.67	2.67	3.73	3.73
Z **(m)**	0.21	2.07	0.21	1.14	2.07	0.21	2.07

omnidirectional transducers Delta Ohm HD103t with the accuracy of ±0.04 m/s in the range of 0–0.99 m/s, and ±0.2 m/s in the range of 1–5 m/s. For relative humidity measurements, an EE Elektronik sensor of J type was used. The accuracy of this sensor is 2.7% in the range above 90% RH and 1.5% below 90% RH. The air temperature in the bulk of cabbage was measured with T-type thermocouples Czaki with a precision of ±0.2 K.

Thermal conditions in the cold storage chamber were changing constantly mainly because of the requirements to defrost the air cooler. The defrost cycle was performed two times a day and was executed by the electric heaters. The fans were stopped at this time. However, during most periods of time, the conditions in the chamber were stable. The measured velocities at levels $V1$–$V5$ during 6 runs of the transducers (approx. 12 hours) are presented as a function of time in Fig. 4. Data collected at this time were selected after averaging for the purpose of the comparison with theoretical prediction obtained for the steady state conditions.

Cooling units are equipped with fans mounted either at the inlet or at the outflow from the chamber. The second location creates important problems for simulations due to difficulties in modelling the details of the jets flowing out from the fans, their

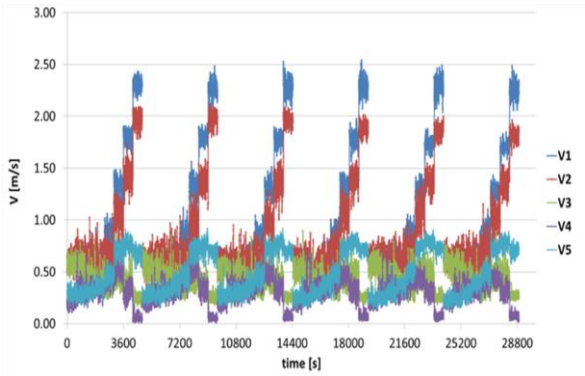

Fig. 4.Velocities measured by the mobile measurement system *vs.* time.

shapes and their swirls. They are the first important factor affecting the flow pattern above the vegetable bed. The other difficulty is the selection of the model of turbulence since this has an impact on the way the air jets flow out of the cooler and interact with each other and with the surroundings. In the present paper, the SST model of turbulence was selected because of its better ability to represent the airflow above the bed. Several models were tested, i.e. the standard model k–ε, RNG k–ε, realizable k–ε, k–ω SST, and SAS. The realizable k–ε and k–ω SST models occurred as the most promising. The realizable k–ε model was slightly better in representing the velocity distribution at the elevations *V1* and *V2* than the SST model, but it was not able to reproduce the velocity profile at *V3*, *V4* and *V5* elevations. Three interfering jets have formed one stream with a contraction near the wall opposite to the cooler, see Fig. 5b. However, the free stream above the bulk is quite wide not too far from the cooler, which may be indicated by the results of measurements collected at *V5* level, see Fig. 6e. The k–ω SST model was the only one which managed to form the air jets wide enough to get close to experimental results obtained at *V5* level, see Fig. 5a.

The experimental and calculated velocities with the use of k–ω SST model of turbulence are compared in Figs. 6–10 for various velocity measurement levels *V1* to *V5* indicated in Fig. 2. The experimental results shown in Figs. 6–10 include the lowest and the highest velocity readings at each grid point. As it can be seen, most of the numerical results lie exactly in the experimental range, however, part of them fall beyond this range, especially at *V3* level. Numerical results of the velocity distribution are shown in Fig. 11. Based on these results, the Coanda effect is seen at which the air jet is attached to and detached from the ceiling and the top of the vegetable bulk. Its shape strongly affects the results at *V1* and *V3* levels. The velocity magnitude at *V3* level depends also on the disturbances caused by the guide of the measurement system. The results obtained for *V2* and *V4* levels seem to be in better agreement with experimental data. The reason for better agreement is the fact that this was a less dynamic region. Figures 6–10 show that the range of velocity readings taken at the same position is fairly wide. That means that the air flow in the stream blown out by

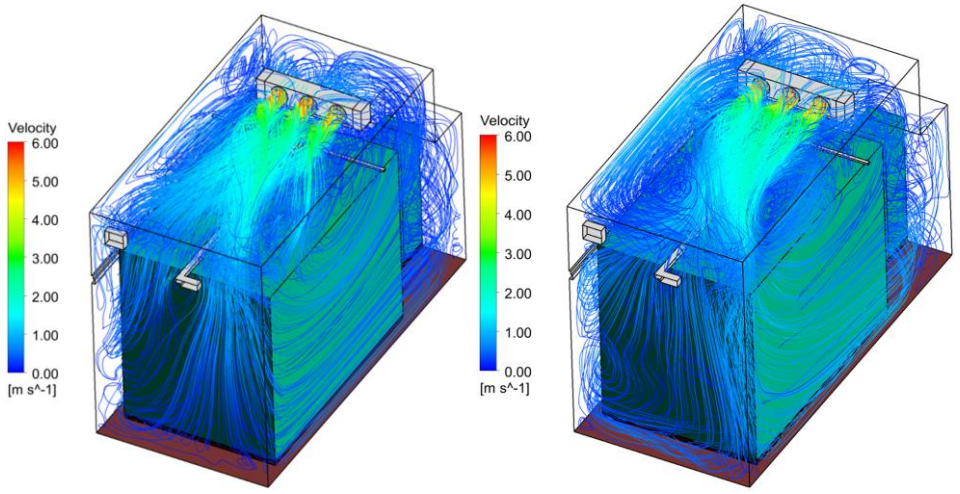

a) b)

Fig. 5. Streamlines in the chamber for two models of turbulence: a) k–ω SST, b) realizable k–ε.

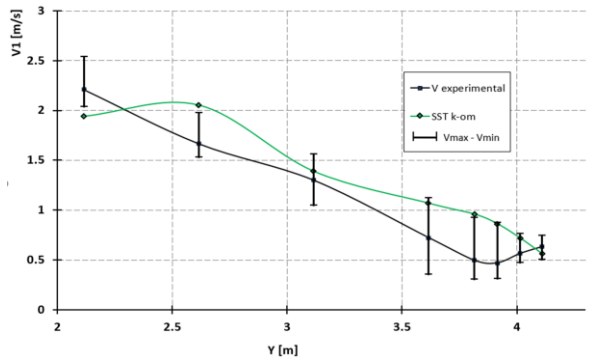

Fig. 6. Experimental and calculated velocities at *V1* level.

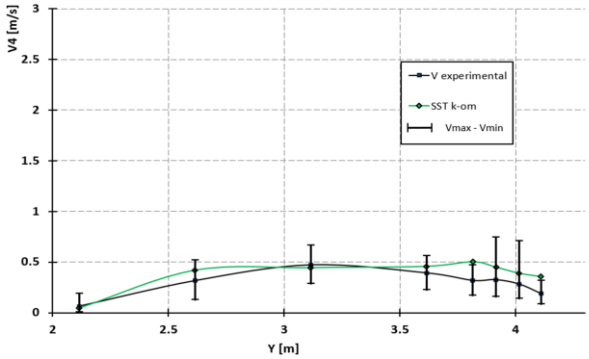

Fig. 9. Experimental and calculated velocities at *V4* level.

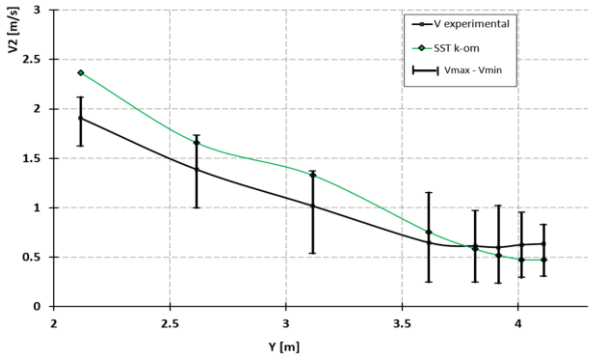

Fig. 7. Experimental and calculated velocities at *V2* level.

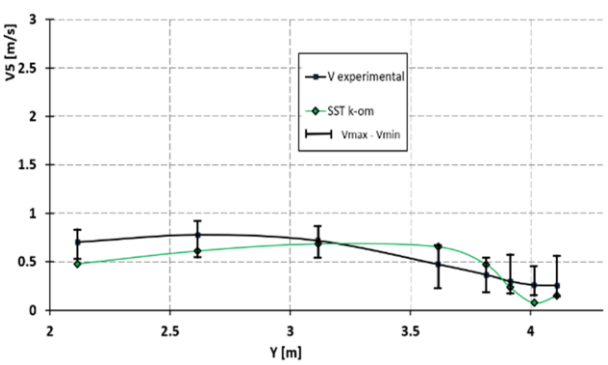

Fig. 10. Experimental and calculated velocities at *V5* level.

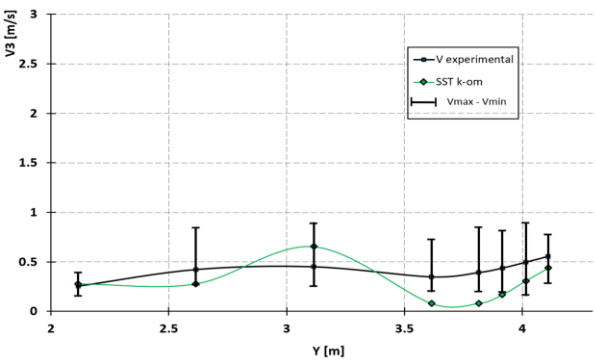

Fig. 8. Experimental and calculated velocities at *V3* level.

the fans is highly turbulent and unstable, and the instantaneous velocity fluctuates continuously around the mean value.

The interfering jets reach the vegetable bulk top surface and the supporting elements of the measurement system. Thus, the stationary process assumed here may be only a quite rough approximation of a real flow that occurs in such a complex system. The comparison shows that further research is required in modelling the air stream from the cooler. The k–ω SST turbulence model proved to be the best one from all the RANS models tested. However, the other time dependent models should be considered in future research, bearing in mind that the use of the SAS model has made no significant improvement.

From our own experience, we can conclude that modelling the physical properties of the outflow from the fans is equally important as modelling the turbulence, because of its great impact on the Coanda effect. An improper divergence angle or jet swirling may have a great impact on the air flow causing gross errors. The obtained results reveal that improvements in modelling of the outflow and turbulence require joint treatment as a single task, which is a very tedious and laborious process.

Table 4 presents the comparison of experimental results and predicted numerical results in terms of relative humidity of air and temperature in the vegetable bulk. Symbols δ_{RH} and δ_t denote mean relative differences between computed and measured values. The best agreement between calculated and experimental results of the relative humidity occurs to be at 7 and 8 verticals, i.e. at the points located below the main stream of air. Based on these results it can be stated that models of transpiration and respiration of vegetables, their coupling with processes occurring in the air cooler as well as the air flow in the vegetable bed are the most crucial issues affecting the relative humidity distribution. Other correlations than those used in this study may better predict the relative humidity distributions. Another factor that is not taken into account in the present model but potentially influencing the results is the freezing of water in the cooler. Accumulation of ice is a serious problem in the real operation of air coolers, requiring periodic defrosting which, in turn, disturbs thermal equilibrium in the chamber and produces a serious impact on the measurements executed even long after the defrost process [41]. During the measurements performed in this case, the air cooler was free of frost, as indicated by the level of velocity magnitude in Fig. 4. In the case of frost accumulation at the air cooler surface, the velocity gradually decreases in time, because of a gradually increasing drag.

Experiments show that the loss-in-weight caused by the drying process after 90-day storage depends on the location in the chamber. The greatest loss of about 11% was obtained in the external rows of the vegetable bulk (at the corner of the bulk opposite to the cooler). This loss is decreasing significantly in the direction of the cooler up to 5% in the column of boxes located at the corner under the cooler. The least shrinkage due to the drying process (about 2−3%) occurred in the column of boxes located in the middle of the bulk and in the column located just under the cooler (about 5%). The overall humidity of air in the jet blown by the fans was moderately low, about 88−89 % (see Table 4), and this was the reason for the shrinkage due to the drying process that occurred at the sides of the bulk most ventilated by the air.

In the middle of the bulk and near the cooler, the lower air flow in the bulk indicated in Fig. 7 did not disturb the humidity generated by transpiration of the cabbage, which resulted in lower shrinkage in these areas.

Based on the calculated velocity and relative humidity distributions presented in Figs. 11 and. 12, the areas in the bulk near the side opposite the cooler, its left and right sides, and the top of the bed − are the most ventilated places of the cabbage bed. Although they have a lower temperature (see Fig. 13), the relative humidity there is lower than in the middle of the bulk. This is a result of higher transpiration caused by the intensive air flow. The water vapour sources distribution S_v, which is shown in Fig. 14, illustrates the process of transpiration of the stored vegetables.

The areas of the greatest magnitude of S_v cover the areas of the least magnitudes of relative humidity and the areas of the highest velocities in the vegetable bulk. The computed water vapour generation rate in the whole bulk was equal to 0.124 kg/h, which after 90-day storage gives a mass loss of 8.8%. This result as well as the relative humidity and S_v distributions prove not only the quali-

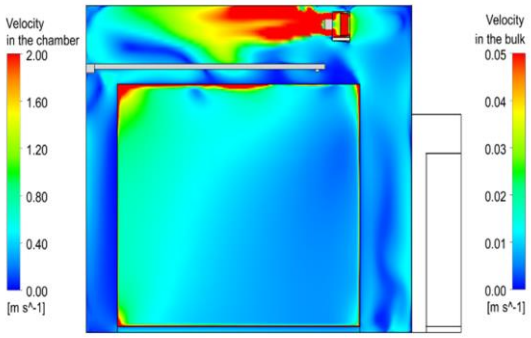

Fig. 11. Velocity distribution in the mid-plane (X = 0.99 m).

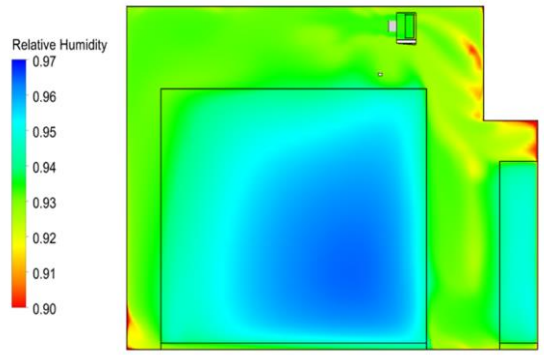

Fig. 12. Relative humidity distribution in the section of the chamber through the fan 1 (X = 0.64 m).

Table 4. Experimental results vs. calculated results.

	Relative humidity of air at RH level (%)								Air temperature in the bulk (K)						
	1	2	3	4	5	6	7	8	1	2	3	4	5	6	7
Exp. values	88.4	88.2	88.0	87.9	87.2	89.1	89.7	88.8	274.36	274.36	274.13	273.93	273.93	274.00	273.94
Calc. values	93.20	93.20	93.20	93.19	93.20	93.22	93.22	93.19	274.33	274.32	274.31	274.32	274.28	274.15	274.19
δ_{RH} (%)	5.43	5.67	5.90	6.02	6.88	4.62	3.92	4.94	–	–	–	–	–	–	–
δ_t (%)	–	–	–	–	–	–	–	–	0.01	0.02	0.07	0.14	0.13	0.06	0.09

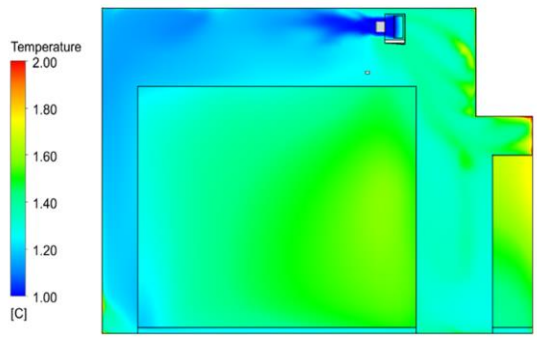

Fig. 13. Temperature distribution in the section of the chamber

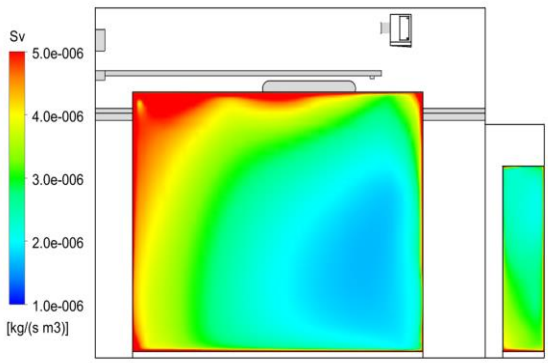

Fig. 14. The distribution of water vapour sources S_v due to transpiration of the cabbage in the section of the chamber through the fan 1 (X = 0.64 m).

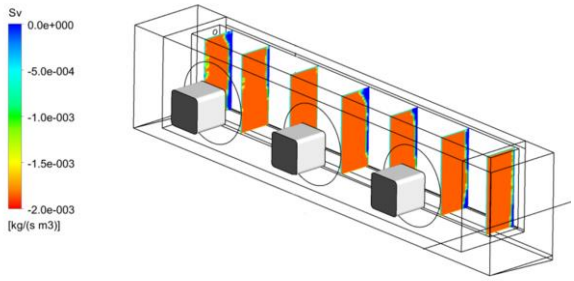

Fig. 15. Condensation rate distribution in the heat exchanger.

tative, but also quantitative reasonable agreement of experimental and computed results, and confirm the validity of the model.

Condensation occurred in the air cooler evaluated as the volumetric water vapour sinks distribution is shown in Fig. 15. The regions where condensation starts are clearly visualised by the sharp boundaries between blue and red colours. The overall condensation rate was equal to 0.116 kg/h, which gives an imbalance of 6.5% between the water vapour generation and destruction in the whole cold storage chamber.

Despite the moderate agreement between numerical and experimental results of velocity, the relative humidity and air temperatures in the vegetable bulk well correspond to each other, see Table 4. The highest temperature difference between experimental data and calculated results was found to be 0.39 K at point *Tp4* located in the middle of the bulk.

The influence of airflow outside the bulk on the conditions inside the bulk is not as large as it was expected. The temperature distribution at the plane cutting the fan 1 (X = 0.64 m) of air in a free space of the chamber and air inside the vegetable bulk is presented in Fig. 13. The greatest temperature was obtained in the boxes in the antechamber as a result of poor ventilation. The impact of heat transfer through outer walls and the highest respiration of the vegetables is presented in Fig. 16. In the main bulk the maximum vegetable temperature was inside the bulk beneath the cooler, where the air penetration was the poorest and the respiretion at its highest. The range of spatial differences of respiratory heat generation rates was very narrow due to small temperature differences in the bulk. This means that the air flow has the greatest impact on the stored vegetable temperature.

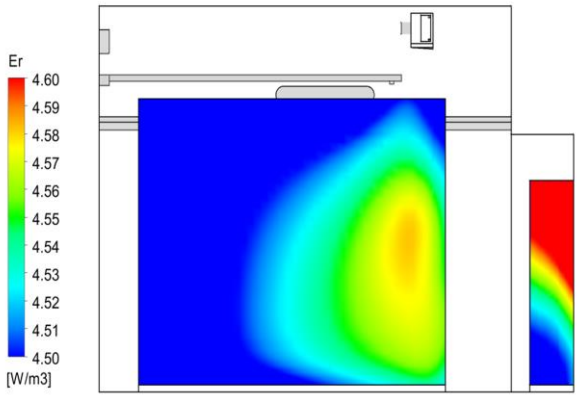

Fig. 16. Respiratory heat generation rate distribution in the section of the chamber through the fan 1 (X = 0.64m).

The heat transfer coefficient between air and cabbage was found to be in the range of 1−7 W/(m^{2}K) and reached the greatest values in the areas of the highest velocities, see Fig. 17. The heat transfer coefficient distribution in the heat exchanger was very uniform. It ranged between 32 W/(m^{2}K) and 34 W/(m^{2}K). The total cooling capacity at the steady-state operation conditions was found to be 256.3 W which is much less than the nominal capacity of the cooler 1148 W declared by the manufacturer. The flow rate of air was equal to 0.307 m^3/s (1105.3 m^3/h), i.e. exactly equal to the nominal data.

5. Conclusions

The following conclusions can be drawn based on the presented results:

- Postharvest life processes of the vegetable bed and heat transfer in the bulk should be considered together with heat and mass transfer in the cooling unit as one computational task;
- The coupling between the vapour production in the bulk and condensation in the cooler is the most distinctive featu-

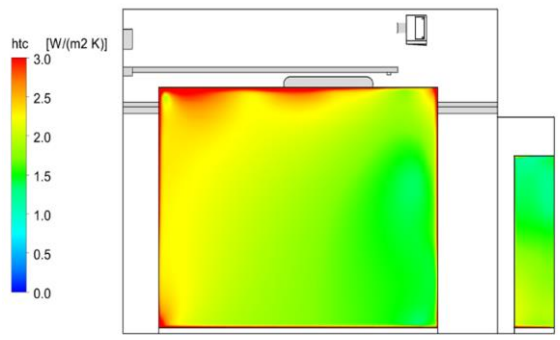

Fig. 17. Contour map of convective heat transfer coefficient between cabbage and air in the section of the chamber through the fan 1 (X = 0.64 m).

re of the model. This feature is vitally important for operation under conditions close to saturation;

- The proper modelling is a complex task that requires the thermal non-equilibrium approach, supported by UDFs. In this paper, the porous media were applied both to the bulk of vegetables and to the air cooler;
- Numerical simulations well predict the relative humidity of air and temperature. The mean relative differences between the results were in the range of 3−7% for the relative humidity and less than 0.2 % for the temperature;
- The heat transfer coefficient between the air and cabbage predicted by numerical simulations was found to be in the range of 1−7 W/(m^{2}K);
- Further works will involve an improved model of prediction of the cooling capacity, including heat transfer between the air side and the inside of the exchanger tubes, and the frosting on the tubes and fins. Further research has also to be done in order to include in the model the biological processes that occur in the vegetables that is still open issue.

Acknowledgements

The research results presented in the paper are supported by the Project No. WZ/WM-IIM/2/2023 supported by the Ministry of Science and Higher Education, Poland.

References

[1] Tian, X., Engel, B.A., Qian, H., Hua, E., Sun, S., & Wang, Y. (2021).Will reaching the maximum achievable yield potential meet future global food demand? *Journal of Cleaner Production*, 294, 126285. doi: 10.1016/j.jclepro.2021.126285

[2] Glaros, A., Marquis, S., Major, C., Quarshie, P., Ashton, L., Green, A.G., Kc, K.B., Newman, L., Newell, R., Yada, R.Y., & Fraser, E. (2022). Horizon scanning and review of the impact of five food and food production models for the global food system in 2050. *Trends in Food Science & Technology*, 119, 550–564. doi: 10.1016/j.tifs.2021.11.013

[3] Bournet, P.E, & Rojano, F. (2022). Advances of Computational Fluid Dynamics (CFD) applications in agricultural building modelling: Research, applications and challenges. *Computers and Electronics in Agriculture*, 201, 107277. doi: 10.1016/j.compag.2022.107277

[4] Janusz, S., Szudarek, M., Rudniak, L., & Borcuch M. (2023). Analysis of heat and mass transfer in an adsorption bed using CFD methods. *Archives of Thermodynamics*, 44(2), 177–194. doi: 10.24425/ather.2023.146564

[5] Hoang, H., Duret, S., Flick, D., & Laguerre, O. (2015). Preliminary study of airflow and heat transfer in a cold room filled with apple pallets: Comparison between two modelling approaches and experimental results. *Applied Thermal Engineering*, 76, 367−381. doi: 10.1016/j.applthermaleng.2014.11.012

[6] Krawczyk, K., & Badyda, K. (2011). Two-dimensional CFD modeling of the heat and mass transfer process during sewage sludge drying in a solar dryer. *Archives of Thermodynamics*, 32(4), 3–16. doi: 10.2478/v10173-011-0028-y

[7] Han, J.W., Zhao, C.J., Yang, X.T., Qian, J.P., & Fan, B.L. (2015). Computational modelling of airflow and heat transfer in a vented box during cooling: Optimal package design. *Applied Thermal Engineering*, 91, 883−893. doi: 10.1016/j.applthermaleng.2015.08.060

[8] Nalbandia, H., Seiiedlou, S., Ghasemzadeh H.R., & Rangbar, F. (2016). Innovative parallel airflow system for forced-air cooling of strawberries. *Food and Bioproducts Processing*, 100(A), 440–449. doi: 10.1016/j.fbp.2016.09.002

[9] Defraeye, T., Lambrecht, R., Delele, M.A., Tsige, A.A., Opara, U.L., Cronjé, P., Verboven, P., & Nicolai, B. (2014). Forced-convective cooling of citrus fruit: Cooling conditions and energy consumption in relation to package design. *Journal of Food Engineering*, 121, 118–127. doi: 10.1016/j.jfoodeng.2013.08.021

[10] Zhang, R., & Long, J. (2017). Study on drying uniformity of static small-sized drying box for fruits and vegetables. *Procedia Engineering*, 205, 2615–2622. doi: 10.1016/j.proeng.2017.10.201

[11] Gautam, K.R., Rong, L., Iqbal, A., & Zhang, G. (2021). Full-scale CFD simulation of commercial pig building and comparison with porous media approximation of animal occupied zone. *Computers and Electronics in Agriculture*, 186, 106206. doi: 10.1016/j.compag.2021.106206

[12] Doumbia, E.M., Janke, D., Yi, Q., Amon, T., Kriegel, M., & Hempel, S. (2021). CFD modelling of an animal occupied zone using an anisotropic porous medium model with velocity depended resistance parameters. *Computers and Electronics in Agriculture*, 181 105950. doi: 10.1016/j.compag.2020.105950

[13] Verboven, P., Hoang, M.L., Baelmans, L., & Nicolai, B.M. (2004). Airflow through beds of apples and Chicory roots. *Biosystems Engineering*, 88(1), 117−125. doi: 10.1016/j.biosystemseng. 2004.02.002

[14] Nahor, H.B., Hoang, M.L., Verboven, P., Baelmans, M., & Nicolai B.M. (2005). CFD model of the airflow, heat and mass transfer in cool stores. *International Journal of Refrigeration*, 28(3), 368−380. doi: 10.1016/j.ijrefrig.2004.08.014

[15] Mirade, P.-S., Rougier, T., Daudin, J.-D., Picque, D., & Corrieu, G. (2006). Effect of design of blowing duct on ventilation homogeneity around cheeses in a ripening chamber. *Journal of Food Engineering*, 75(1) 59−70. doi: 10.1016/j.jfoodeng.2005. 03.053

[16] Hoang, M.L., Verboven, P., De Baerdemaeker, J., & Nicolai, B.M. (2000). Analysis of the air flow in a cold store by means of computational fluid dynamics. *International Journal of Refrigeration*, 23(2), 127−140. doi: 10.1016/S0140-7007(99) 00043-2

[17] Tapsoba, M., Moureh, J., & Flick, D. (2006). Airflow patterns in an enclosure loaded with slotted pallets. *International Journal of Refrigeration*, 29(6), 899−910. doi: 10.1016/j.ijrefrig.2006.01.011

[18] Tapsoba, M., Moureh, J., & Flick, D. (2007). Airflow patterns inside slotted obstacles in a ventilated enclosure. *Computers & Fluids*, 36(5), 935−948. doi: 10.1016/j.compfluid.2006.04.002
[19] Moureh, J., Menia, N., & Flick, D. (2002). Numerical and experimental study of airflow in a typical refrigerated truck configuration loaded with pallets. *Computers and Electronics in Agriculture*, 34(1-3), 25−42. doi: 10.1016/S0168-1699(01) 00178-8
[20] Moureh, J., Tapsoba, M., & Flick, D. (2009). Airflow in a slot-ventilated enclosure partially filled with porous boxes: Part I – Measurements and simulations in the clear region. *Computers & Fluids*, 38(2), 194−205. doi: 10.1016/j.compfluid.2008.02.006
[21] Moureh, J., Tapsoba, S., & Flick, D. (2009). Airflow in a slot-ventilated enclosure partially filled with porous boxes: Part II − Measurements and simulations within porous boxes. *Computers & Fluids*, 38(2), 206−220. doi: 10.1016/j.compfluid.2008.02.007
[22] Moureh, J., & Flick, D. (2004). Airflow pattern and temperature distribution in a typical refrigerated truck configuration loaded with pallets. *International Journal of Refrigeration*, 27(5), 464−474. doi: 10.1016/j.ijrefrig.2004.03.003
[23] Ferrua, M.J., & Singh, R.P. (2009). Modeling the forced-air cooling process of fresh strawberry packages, Part I: Numerical model. *International Journal of Refrigeration*, 32(2), 335−348. doi: 10.1016/j.ijrefrig.2008.04.010
[24] Ferrua, M.J., & Singh, R.P. (2009). Modeling the forced-air cooling process of fresh strawberry packages, Part II: Experimental validation of the flow model. *International Journal of Refrigeration*, 32(2), 349−358. doi: 10.1016/j.ijrefrig.2008.04. 009
[25] Delele, M.A., Schenk, A., Tijskens, E., Ramon, H., Nicolai, B.M., & Verboven, P. (2009). Optimization of the humidification of cold stores by pressurized water atomizers based on a multi-scale CFD model. *Journal of Food Engineering*, 91(2), 228−239. doi: 10.1016/j.jfoodeng.2008.08.027
[26] Delele, M.A., Schenk, A., Ramon, H., Nicolai, B.M., & Verboven, P. (2009). Evaluation of a chicory root cold store humidification system using computational fluid dynamics. *Journal of Food Engineering*, 94(1), 110−121. doi: 10.1016/j.jfoodeng. 2009.03.004
[27] Chourasia, M.K., & Goswami, T.K. (2007). Steady state CFD modeling of airflow, heat transfer and moisture loss in a commercial potato cold store. *International Journal of Refrigeration*, 30(4), 672−689. doi: 10.1016/j.ijrefrig.2006.10. 002
[28] Xu, Y., & Burfoot, D. (1999). Simulating the bulk storage of foodstuffs. *Journal of Food Engineering*, 39(1), 23−29. doi: 10.1016/S0260-8774(98)00139-3
[29] Ansys Inc. (2015). *Ansys Fluent Theory Guide*, Release 16.0. Ansys Inc., Canonsburg.
[30] Bohojło-Wiśniewska, A. (2015). Numerical modelling of humid airflow around a porous body. *Acta Mechanica et Automatica*, 9(3), 161−166. doi: 10.1515/ama-2015-0027
[31] Śmierciew, K., Kołodziejczyk, M., Gagan J., & Butrymowicz D. (2018). Numerical modeling of fin heat exchanger in application to cold storage. *Heat Transfer Engineering*, 39(10), 874−884. doi: 10.1080/01457632.2017.1338862
[32] Butrymowicz, D., Łapiński, A., Gagan, J., & Śmierciew, K. (2016). Application of single blow technique for heat transfer measurement in packed bed of vegetables. *16th International Refrigeration and Air Conditioning Conference at Purdue*, 11–14 July, West Lafayette, USA.
[33] Becker, B.R., & Fricke, B.A. (1996). Simulation of moisture loss and heat loads in refrigerated storage of fruits and vegetables. *New Developments in Refrigeration for food Safety and Quality* (pp. 210−221), 2–4 October, Lexington, USA, International Institute of Refrigeration and American Society of Agricultural Engineers.
[34] Bird, R.B., Stewart, W.E., & Lightfoot, E.N. (2002). *Transport Phenomena*. John Wiley, New York.
[35] Nguyen, T.A., Verboven, P., Schenk, A., & Nicolai, B.M. (2007). Prediction of water loss from pears during controlled atmosphere storage a affected by relative humidity. *Journal of Food Engineering*, 83(2), 149−155. doi: 10.1016/j.jfoodeng.2007.02. 015
[36] Dehghannya, J., Ngadi, M., & Vigneault, C. (2008). Simultaneous aerodynamic and thermal analysis during cooling of stacked spheres inside ventilated packages. *Chemical Engineering Technology*, 31, (11), 1651−1659. doi: 10.1002/ceat.200800290
[37] Becker, B.R., & Fricke, B.A. (1996). Transpiration and respiration of fruits and vegetables. *New Developments in Refrigeration for Food Safety and Quality* (pp. 110−121), 2–4 October, Lexington, USA, International Institute of Refrigeration and American Society of Agricultural Engineers.
[38] ASHRAE (2006). Thermal properties of foods (Chap. 9). In *Handbook – Refrigeration*, (pp. 9.1−9.31). Inch-Pound Edition, American Society of Heating, Refrigerating and Air-Conditioning Engineers, Inc.
[39] Ma, X., Ding, G., Zhang, Y., & Wang K. (2007). Airside heat transfer and friction characteristics for enhanced fin-and-tube heat exchanger with hydrophilic coating under wet conditions. *International Journal of Refrigeration*, 30(7), 1153−1167. doi: 10.1016/j.ijrefrig.2007.03.001
[40] Kondjoyan, A. (2006). A review on surface heat and mass transfer coefficients during air chilling and storage of food products. *International Journal of Refrigeration*, 29(6), 863−875 doi: 10.1016/j.ijrefrig.2006.02.005
[41] Kołodziejczyk M., Butrymowicz D., Gagan J., & Śmierciew K. (2016). Investigations of Chinese cabbage cold storage chamber operation. *16th International Refrigeration and Air Conditioning Conference at Purdue*, 11–14 July, West Lafayette, USA